J Polym Res (2011) 18:2367–2378
DOI 10.1007/s10965-011-9651-1

ORIGINAL PAPER

Impact of filler geometry and surface chemistry on the degree of reinforcement and thermal stability of nitrile rubber nanocomposites

P. C. Thomas · Selvin P. Thomas · Gejo George · Sabu Thomas · Joseph Kuruvilla

Received: 6 November 2010 / Accepted: 22 June 2011 / Published online: 6 July 2011

Abstract The morphological, mechanical, and thermal stability of Nitrile rubber nanocomposites reinforced with fillers such as layered silicate (LS), calcium phosphate (CP) and titanium dioxide (TO) having different particle size and chemical nature were analyzed. The results revealed that the filler geometry played an important role on the mechanical and thermal stability of the composites. Calcium phosphate and titanium dioxide filled systems showed comparatively better mechanical and thermal stability compared to neat rubber. The activation energy needed for the thermal degradation was found to be higher for layered silicate filled system. DSC (Differential Scanning Calorimetry) analysis revealed a change in the T_g values as a result of the addition of fillers. This was more prominent with the case of layered silicate filler addition in comparison with calcium phosphate and titanium dioxide. The heat capacity values of the nanocomposites were carefully evaluated. The (ΔCp) with values obtained for different nanocomposites were correlated with the degree of reinforcement. It can be assumed that more polymer chains are attached on to the surface of the filler and there exists an immobilized layer around the filler surface and the layers do not take part in the relaxation process. The FTIR spectrum of the different samples highlighted the possible filler matrix interaction. The filler dispersion and aggregation in the polymer matrix were analyzed using X-ray diffraction studies (XRD), transmission electron microscopy (TEM), and atomic force microscopy (AFM).

Keywords Nitrile rubber · Nanocomposites · Layered silicate · Calcium phosphate · Titanium dioxide · Thermogrvimetric analysis · Differential scanning calorimetry

P. C. Thomas · G. George
Research and Postgraduate Department of Chemistry, St. Berchmans' College, Changanacherry, Kerala 686 101, India

S. P. Thomas
Department of Chemical Engineering, King Fahd University of Petroleum & Minerals, Dhahran 31261, Kingdom of Saudi Arabia

S. Thomas
School of Chemical Sciences, Mahatma Gandhi University, Kottayam, Kerala 686 560, India

J. Kuruvilla (✉)
Department of Chemistry, Indian Institute of Space Science and Technology, Trivandrum, Kerala, India
e-mail: kjoseph.iist@gmail.com

Introduction

In recent years, organic–inorganic nanometer composites have attracted great interest from researchers since they frequently exhibit unexpected hybrid properties synergistically derived from two components. One of the most promising composites systems would be hybrids based on organic polymers and inorganic clay minerals consisting of layered structure, which belong to the general family of 2:1 layered silicates [1]. There is a great interest in polymer-clay nanocomposites. Polymer–clay nanocomposites have been shown to exhibit a significant increase in thermal stability [2]. For engineering applications of polymeric materials it is very essential to get the information about thermal stability and degradation. The dispersion of the clay within the polymer has significant influence on the thermal properties of the material due to characteristic structure of layers in polymer matrix and nanoscopic dimensions of

filler particles. The level of surface activity of the filler directly influences the thermal stability of the resulting compound. In general, filler loading in polymers can enhance the tensile as well as thermal properties to a considerable extent. The poly (methyl methacrylate) (PMMA)-montmorillonite (MMT) clay nanocomposites were synthesized by two different techniques namely, ultrasonic mixing and magnetic stirring by Rajan et al. [3] and found that the thermal stability was increased by nearly 30% for ultrasonic mixing than that by magnetic stirring due to very fine dispersion of the clay in the matrix. Bourbigot et al. [4] studied the thermal stability of polystyrene nanocomposites and found that the addition of nanoclay increases the thermal stability of the PS/clay composites. The thermogravimetric analysis of self-assembled poly(vinyl alcohol)/silica (PVA/SiO2) by Peng et al. [5] showed that the nanocomposite significantly outperforms the pure PVA in the thermal resistance . Mohan and co-workers [6] investigated the thermal properties of Diglycidyl ether of bisphenol-A (DGEBA) epoxy resin system (diamino-diphenylmethane (DDM) hardener filled individually with organoclay and unmodified clay and found that organoclay fillers exhibited good thermal properties than that of epoxy with unmodified clay fillers. Ma et al. [7] observed that the glass transition temperature and thermal degradation temperature of zinc oxide/polystyrene nanocomposite increased with ZnO content. The thermal stability of the NR/SiO_2 nanocomposite were studied and found that the degradation temperatures, reaction activation energy, and reaction order of the nanocomposite are markedly higher than those of the pure NR, due to significant retardant effect of the SiO_2 nanoparticles [8]. Studies on the thermal behavior and flammability properties of the heterophasic polypropylene- (ethylene-propylene) copolymer (PP-EP)/poly(ethylene vinyl acetate) (EVA)/montmorillonite nanocomposite by Valera et al. [9] revealed that nanoclays retard thermal degradation depending on nanoclay concentration. The retarding process was assigned to the exfoliation and dispersion of the silicate layers which impeded heat diffusion to the macromolecules. The thermal stability of nanofiller reinforced various polymers have been analysed by a number of workers [10–16] and found that the nanocomposites of all polymers exhibited an enhancement in thermal stability with the dispersion of the nano fillers. The enhancement in glass transition temperature and improvement in the thermal stability of NBR/Na-MMT nanocomposites were reported by Kader et al. [17]. Nitrile rubber is one of the most widely used, commercialised and mass produced special purpose elastomer. Because of its good processability, resistance to oil, fuel, and chemicals as well as its good mechanical properties after vulcanization, NBR has found a variety of applications in sealants, hoses, belts, shoes, and brake linings. However, NBR exhibits poor mechanical properties without vulcanization and reinforcing fillers. Therefore, much attention has recently been given to the preparation of nitrile rubber nanocomposites using suitable nanofillers. The nanocomposites derived from nitrile rubber (NBR) have been investigated extensively with respect to morphological and rheological properties [18], mechanical and dynamic mechanical properties [19], gas barrier properties [20, 21], fracture behaviour and cure properties [22, 23]

The present study focused on the morphological, mechanical and thermal behaviour of sulfur vulcanized nitrile rubber in presence of fillers like layered silicate (LS), calcium phosphate (CP) and titanium dioxide (TO). These fillers have different particle size, shape and surface chemistry; hence the impact of these fillers on the morphological, mechanical and thermal behaviour of the polymer matrix (Nitrile rubber) has been studied in this present work.

Experimental

Materials

The nitrile butadiene rubber (NBR) under the trade name (NBR-553) having Mooney viscosity (ML_{1+4} 100°C) 40.00 and bound acrylonitrile content 33.90% was supplied by Apar Industries, Mumbai. The layered silicate (I.44P) was obtained from Nanocor China. Nanomer I.44P is onium ion modified MMT clay containing 60% clay (CAS No. 1318-93-0) and 40% dimethyl dialkyl (C14-18) ammonium organic modifier. Calcium phosphate in the nanometre (particle size 40 nm) range was prepared in our laboratory by Thomas et al. [24] and titanium dioxide under the trade name KEMOX-RC 800PG, having particle size 190 nm was supplied by Kerala Minerals and Metals Ltd (KMML), Kollam, Kerala, India. The compounding ingredients, such as vulcanising agents and accelerators were procured from M/s Bayer India Ltd., Mumbai.

Sample preparation

Different samples were prepared according to the specified formulations given in Table 1. The mixing process was carried out using a laboratory two roll-mixing mill (150mm X 300mm) at a friction ratio 1:1.4. The machine was water cooled during the mixing operation. The compounding was performed at room temperature keeping the nip gap; mill roll speed ratio and the time taken (16 min overall time) same in all the samples. The samples were designated as NBR/TO, NBR/CP and NBR/LS representing various fillers such as TiO_2, $Ca_3(PO_4)_2$ and layered silicate

Table 1 Composition of the NBR nanocomposites

Ingredient	Quantity (phr)
NBR	100
Zinc oxide	5
Stearic acid	1
TDQ	1
CBS	0.75
Sulfur	2
Fillers (LS, CP & TO)	Variable(0,5,10,15,20)

LS: Layered silicate; CP: Calcium phosphate; TO: Titanium dioxide
CBS: N-Cyclohexyl benzothiazole-2-sulphenamide
TDQ: 2,2,4 Trimethyl-1, 2 dihydroquinoline

(MMT) respectively in sulphur vulcanizing system. The fillers were heated in an oven at 100°C for 8 h to remove the moisture, kept in a desiccator and used for the composite preparation. NBR was first masticated for 2 min before the ingredients were added in the same order as mentioned. The samples were cured at 160°C in an electrically heated hydraulic press to their respective cure time (t_{90}) at a pressure of 150 kg/cm^2 to get sheets of thickness 1.5mm (approximately).

Analysis and characterization

The morphology of the cryofractured composites was analyzed by using small angle X-ray scattering (SAXS), transmission electron microscopy (TEM) and atomic force microscopy (AFM) techniques. X-ray diffraction patterns of the nitrile rubber nanocomposites were taken using Ni-filtered Cu-Kα radiation at a generator voltage of 60 kV, and a generator current of 40 mA and wavelength of 0.154 nm at room temperature (Bruker–D 8). Transmission electron micrographs of the samples were taken in a LEO 912 Omega transmission electron microscope with an acceleration voltage of 120kV. The specimens were prepared using an Ultra cut E cryomicrotome. Thin sample specimens of about 100 nm were obtained with a diamond knife at −100°C. Atomic force microscopy was done with Park systems (XE-100 AFM), South Korea. The samples for AFM were prepared by cryogenically fracturing them in liquid nitrogen, and the topographic AFM images were obtained. The FTIR spectra were taken in a Thermo Nicoletet (5700-USA) specrtophotometer.

The curing properties were studied using Elastograph "Vario" 67.98 (Gottfert; Germany) rheometer by placing 7–10 g of the different samples in the heating chamber of the rheometer operated at 160°C. Torque maximum, torque minimum, scorch time and cure time were obtained from the rheometer observations. Separate rheographs were taken for each composition (sample) to get the respective cure time. Tensile and tear tests were performed on dumbbell and crescent shaped specimens according to ASTM standards D 412 and D 624 on Instron 4411(England) UTM at a cross head speed of 500 mm/min and 100 mm/min respectively.

The thermogravimetric analysis of the composites was carried out in Perkin-Elmer TGA analyzer. About 3–5 mg of the samples was thermally degraded in a nitrogen flow of 30cm^{3}min^{-1} in the thermo balance at a heating rate of 10°C min^{-1}. The samples were scanned from 30°C to 600°C at a heating rate of 10°C min^{-1}. From the TGA curves, the thermal degradation characteristics were calculated. The change in glass transition temperature was noticed using Perkin–Elmer DSC thermal analyzer. In this process about 5 mg of the samples were heated from −50°C to 90°C under nitrogen atmosphere with a programmed heating rate of 10°C/min. All TGA and DSC measurements were done in triplicate with high reproducibility.

Results and discussion

Curing behaviour

The vulcanization characteristics are expressed in terms of torque (min), torque (maxi), scorch time t_{s1}, optimum cure time t_{90}, cure rate (t_{90}-t_{s1}) and torque increase. The rheological properties of the gum and nanocomposites at 10 phr (parts per hundred rubber) filler loading (TO, CP and LS) are given in Fig. 1. The increase in maximum and minimum torques as well as their difference is higher in the case of LS and CP filled system compared to TO filled composites. This implies that there is some reinforcement

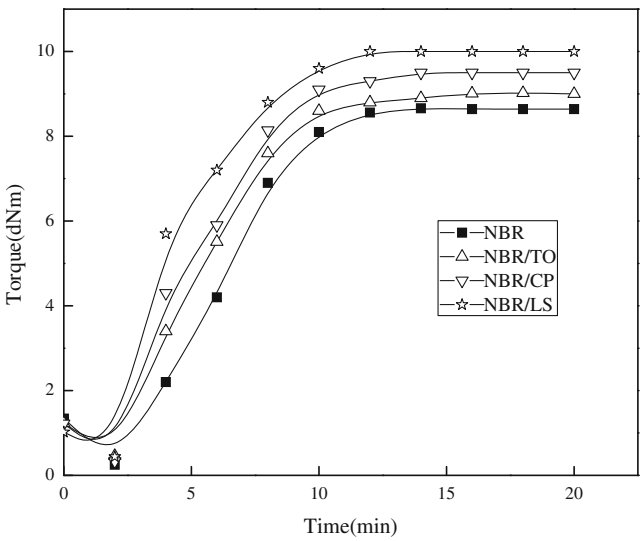

Fig. 1 Cure characteristics of nanocomposites at 10 phr of filler loading

effect for both LS and CP on the polymer matrix. This happens when fillers are intercalated and/or exfoliated. The maximum values torques associated with LS filled system can be attributed to the intercalation/exfoliation of the layered silicate by nitrile rubber matrix [19]. The curing time t_{90} values indicate that both LS and CP accelerates the vulcanization. In the case of LS this effect is observed for other rubbers (Natural Rubber, Chlorobutyl rubber etc.), and this effect is due to the formation of a transitional metal complex in which the sulphur and amine groups of the intercalants participate in the complex formation [25, 26]. The scorch time analysis showed that there is marginal decrease in scorch time as a result of the addition of TO filler and this indicates that the TO filler, as such, has little influence on the cure reactions of nitrile rubber due to their inert chemical nature. However surface modified layered silicate and CP fillers showed comparatively more reduction in the scorch time of the nitrile rubber. These fillers behave like a vulcanizing accelerator for NBR decreasing the scorch time. Such accelerating effect has already been reported by Wu et al. in NBR/organosilicate system [27]. This may be due to the complex formation with amines and sulphur containing compounds which facilitates the formation of elemental sulphur and this is the reason for the slight variation in scorch time and cure time of the filled nitrile rubber systems.

Morphology of the nitrile rubber nanocomposite samples

Figure 2 shows the X-ray diffraction of layered silicate and their NBR hybrids. No peak was observed for pure NBR, indicating its amorphous nature. Layered silicate exhibits a single peak at 2θ of 3.77°. When small amount of LS was incorporated in NBR, peak shifted to 2.12° which is an indication of the fact that the LS is partially exfoliated or intercalated at this particular filler loading. Again at 10 phr layered silicate loading; a single prominent peak appeared at an angle of 2θ of 2.58° which is slightly higher than that observed at 5 phr filler loading. However at higher filler loading (20 phr) peaks were observed at 2.89°, 4.71° and 9.37°. The first peak at 2.89° testifies the intercalation of the polymer matrix in to the layered silicate structure, whereas the two peaks observed at 4.71° and 9.37° are attributed to the de-intercalation or particle agglomeration at higher filler loading. Similar results have been appeared in the literature [19, 27]. The calcium phosphate and titanium dioxide filled systems showed no reflections (2θ>15°).

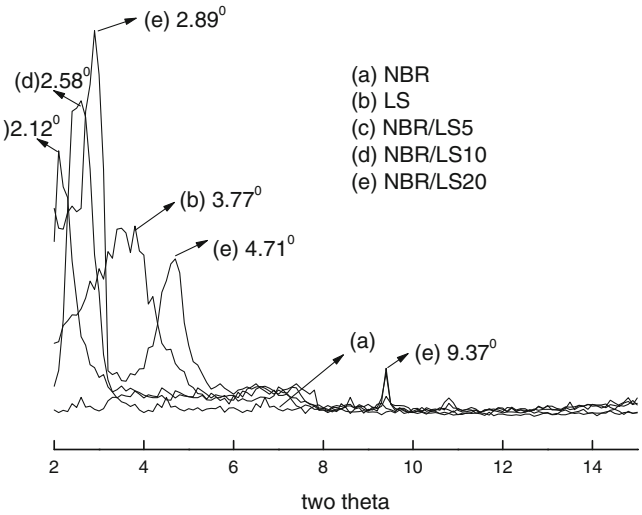

Fig. 2 X-ray diffraction pattern of nitrile rubber nanocomposites

The interaction between the filler and the matrix, which resulted in the exfoliation/intercalation of the matrix between the layers of the filler, can be observed from the TEM pictures of the nanocomposites which are displayed in Fig. 3. These pictures provide clear evidence for the delamination of NBR matrix in the layered silicate. TEM micrograph of NBR/LS nanocomposites at 10 phr reveals that there is minimum agglomeration of the layered silicate in the NBR matrix, and the layered silicate appears to be dispersed more uniformly in comparison with other fillers namely CP and TO. Particle agglomeration is appeared in the NBR/CP and NBR/TO composites, which resulted in the less effective interaction between the polymer matrix and fillers. AFM images of the surfaces of the composites were analyzed to understand filler dispersion behaviour in the matrix. The phase images of the virgin polymer and the composites with different fillers at 10 phr loading were given in Fig. 4a-d. Figure 4a shows the phase image of the neat matrix. It can see seen that the neat matrix shows a smooth surface in comparison with other filler loaded samples. The comparison of surfaces (Fig. 4b-d) revealed that more uniform particle dispersion is associated with layered silicate. Hence it can be concluded that effective filler-matrix interaction follows the order NBR/LS>NBR/CP >NBR/TO

The possible strong interactions or chemical reactions that take place between the filler and the polymer in a polymer nanocomposites can be illustrated with the help of Infrared spectra of the samples [28, 29]. Figure 5 shows FTIR spectra over a frequency range of 900–1,700 cm^{-1} of the nanofillers, cured nanocomposites and pure NBR. Absorption peaks are observed at 970 (C-S not linked to N) and 1250 (C-S linked to N) cm^{-1}, which are characteristic of cured pure NBR compound. The peak at 1,040 cm^{-1} attributed to sulfoxide stretching vibrations. A medium and broad absorption band at approximately 1085cm^{-1} and 1,055 cm^{-1} appears in the spectra indicating that a strong interaction between the hydroxyl group of layered silicates and the curative reaction products exists and which in turn results in a new absorption peak in the NBR nanocomposite. This can be attributed to the strong

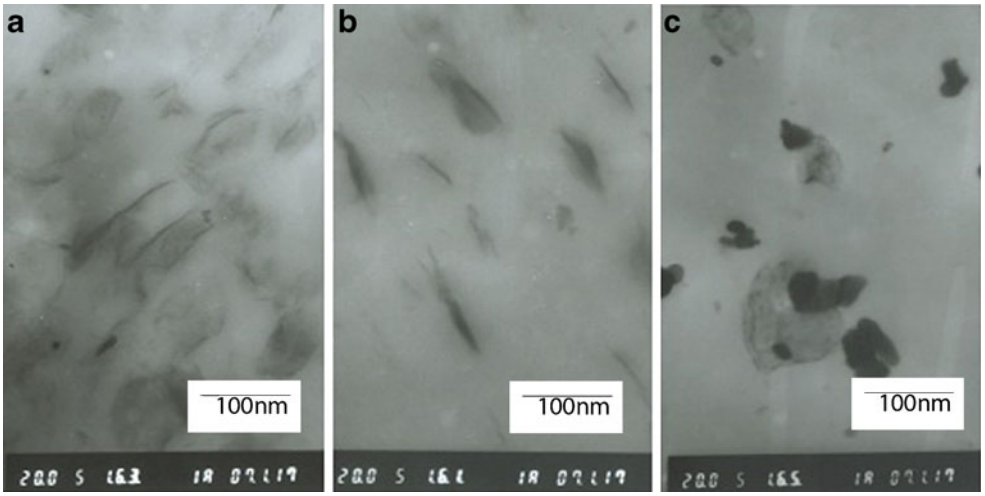

Fig. 3 TEM pictures of nitrile rubber nanocomposites at 10 phr filler loading (**a**) NBR/LS (**b**) NBR/CP and (**c**) NBR/TO

interaction between the intercalated NBR chains and organosilicate layers [30]. In the case of NBR/CP system, there are two peaks appearing at 1,125 cm^{-1} and 1,020 cm^{-1} and this may be due to the strong interaction between CP particles with that of -CN group of nitrile rubber matrix. On closer examination of NBR/TO spectral lines we can see that the spectral lines characteristic for the TO filled system is just ditto of the neat rubber. Hence it can be concluded that there is no effective interaction between the TO filler and the nitrile rubber. This is another reason for the relatively poor property enhancement for the TO filled system.

Tensile and modulus analysis

Figure 6 indicates that the tensile strength is higher for all loadings containing layered silicate in comparison with CP and TO, which is an indication of good intercalation/exfoliation of nitrile rubber segments into the silicate layers. An increase of 348% is noticed in NBR/LS system, which is attributed to a very good filler- matrix interaction in presence of the sulphur-sulphur network [31]. Whereas in NBR/CP system the percentage increase in tensile strength is only 110% and this can be attributed to the fact that in NBR/CP system the CP particles are neither exfoliated nor intercalated and due to this they show very poor binding action with the nitrile rubber segments because of the less availability of surface area per unit volume of the filler. In NBR/TO system, the tensile strength increase is only 84% due to the more spherical nature and increased particle size of TO, which further reduces the surface area per unit volume of the filler available for interaction with the NBR polymer matrix. Thomas et al. studied the mechanical properties of TiO_2 filled polystyrene (PS) and found that the increase in tensile strength is maximum at 5 wt.% addition of TiO_2 [32]. From the tensile variations it can be concluded that the intercalation/exfoliation phenomenon of the polymer matrix is almost negligible with TiO_2 due to the more spherical shape of the filler or due to non-intercalation of the filler particle. The overall tensile performance of different fillers in conventionally vulcanized nitrile rubber is in the order of NBR/LS>NBR/CP >NBR/TO>gum.

Modulus enhancement

The enhancement of modulus at different elongations of the nanocomposite material is shown in Fig. 7. The enhancement can be attributed to the strong intercalation/exfoliation of the layered silicate with the polymer matrix because of its peculiar particle geometry. At 300% elongation NBR/LS system showed an enhancement of 198% whereas at the same conditions NBR/CP showed an increase of 63% and at the same time NBR/TO showed only 22% increase. In all the above three cases the loading was 20phr. From the results it is obvious that the addition of layered silicate resulted in the tremendous increase of modulus due to the nanometric dispersion of the silicate layers giving efficient reinforcement leading to improved stiffness of the material. Since the fillers have different chemical natures, the extent of their interactions with polymer matrix will be of different magnitude, which is clearly depicted in Fig. 7. The high aspect ratio of the layered silicate results in improvement in stiffness of the nanocomposite. In the case of CP and TO, the reinforcing efficiency is less due to spherical nature, which resulted in the minimum availability of surface area of the filler for getting effective contact with the polymer matrix. Yoon et. al [33] reported an enhancement in modulus for NBR/modified MMT with vinyl group nanocomposites as a result of nanometric dispersion of the layered silicate.

Analysis of the thermogravimetric data

Polymeric materials are subjected to various types of degradation ranging from thermal degradation to biodegra-

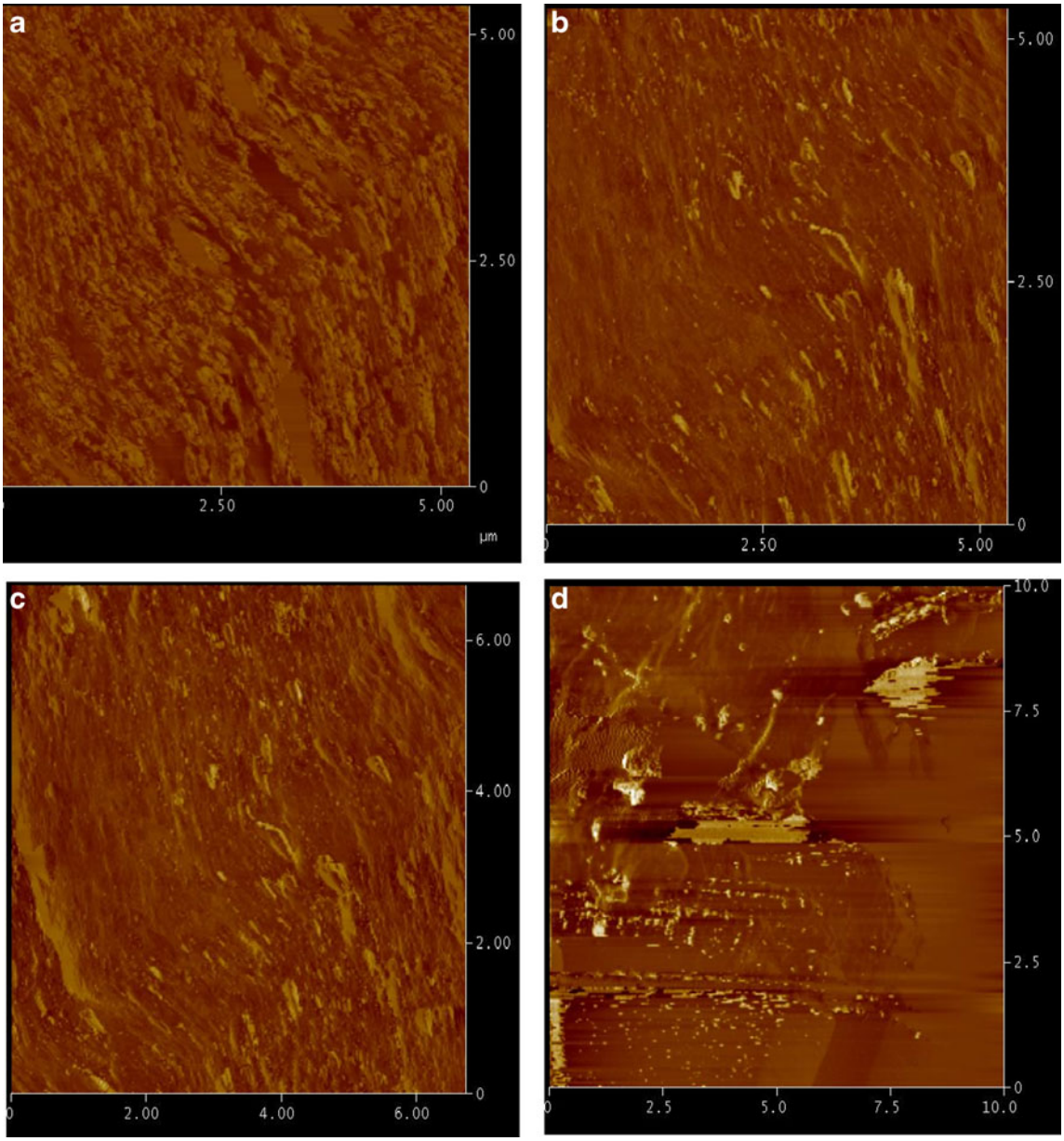

Fig. 4 AFM images of virgin polymer and composites at 10 phr loading (**a**) neat rubber (**b**) NBR/LS (**c**) NBR/CP (**d**) NBR/TO

dation. Thermal degradation studies involve the measurement of the changes in weight of the material as a result of heating in presence of an inert atmosphere or in presence of air/oxygen. One of the most well accepted methods for studying the thermal properties of polymeric materials is the thermogravimetric analysis. The integral (TGA) and derivative (DTG) thermogravimetric curves provide information about thermal stability and extent of degradation of the polymeric material. The heating process brings a lot of changes in the material and finally leaves behind inert residue. In all the cases, at around 100° C, moisture present, if any will be eliminated. Further heating will remove the organic matter and leaving behind the inorganic fillers as residue.

The thermal behaviour (TGA) at the heating range of 30°C to 600°C of the neat polymer and the layered silicate filled samples are shown in Fig. 8. At lower temperature, there is no considerable change in the material behavior of the filled samples and gum. As the temperature increases degradation starts showing enhanced stability of layered silicate filled systems. The degradation of NBR starts at 351°C whereas that of NBR/LS_{20} phr starts at 369°C. This may be due to the intercalation/exfoliation of the polymer matrix with the silicate particles, which resulted in a strong

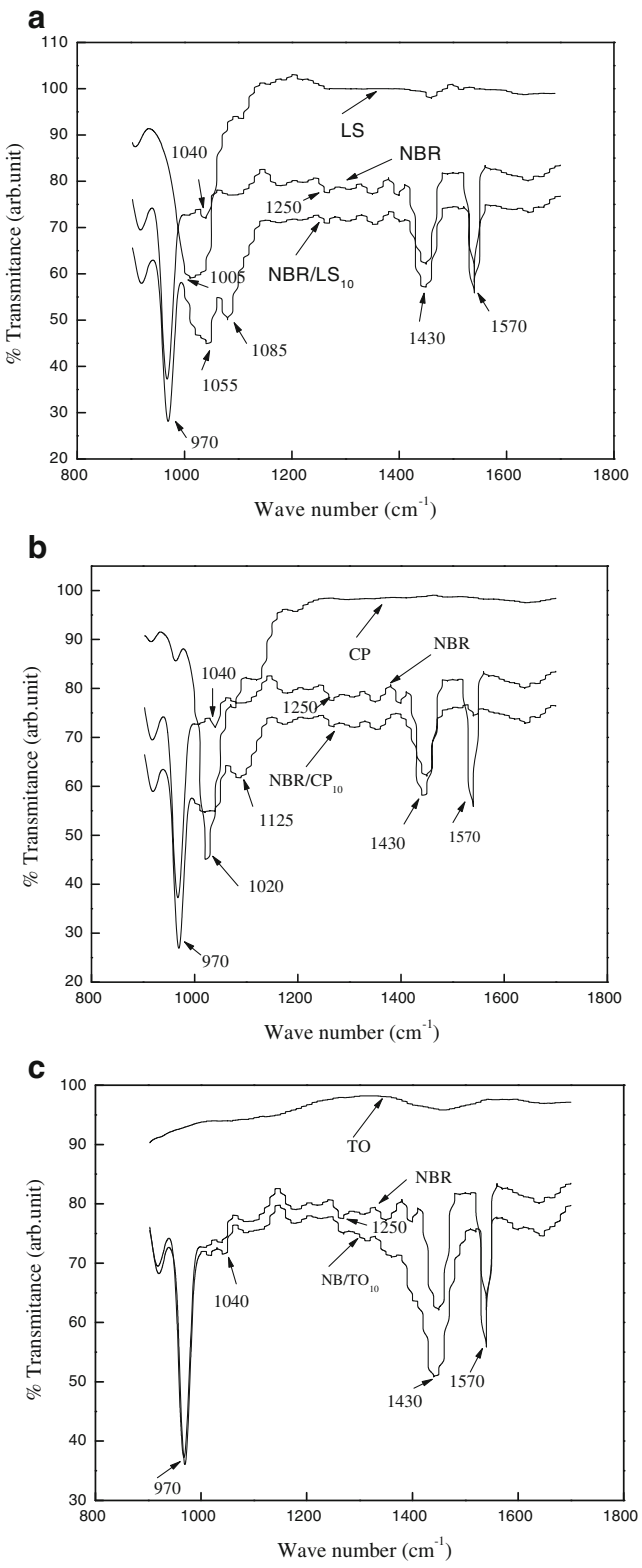

Fig. 5 FTIR spectra of NBR and nanocomposites (**a**) NBR/LS (**b**) NBR/CP and (**c**) NBR/TO

barrier effect, preventing the thermal degradation to a certain extent and this observation is an indication of the fact that NBR/LS 20 is stable up to a temperature of 369°C

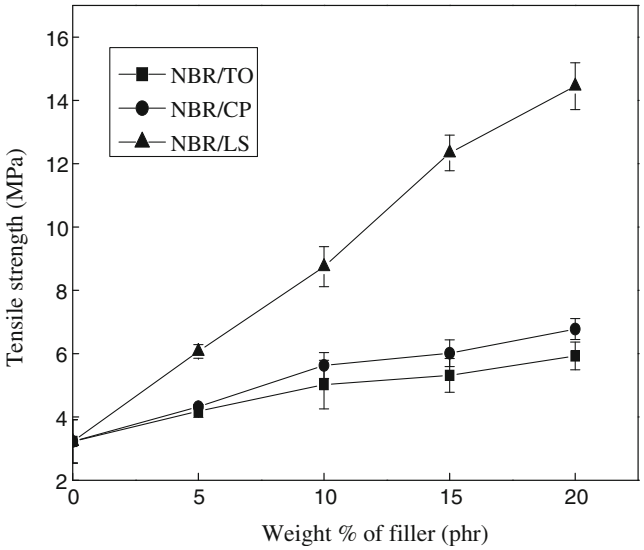

Fig. 6 Variation of tensile strength with filler loading of NBR/TO; NBR/CP and NBR/LS

in nitrogen atmosphere. As a general trend, thermal stability increases with the increase in filler loading but at 15phr and 20phr, nano composites exhibit almost same trend towards thermal stability revealing the fact that higher loading of the filler is not required for thermally stable nitrile rubber system.

The thermal behaviour of CP and TO filled nitrile rubber nanocomposites are shown in Figs. 9 and 10. The curves indicate that the addition of CP and TO fillers to the matrix marginally increased the thermal stability of the polymer. The less effective thermal protection by these fillers in comparison with LS may be due to the minimum availability of surface area which is a measure of length to breadth ratio of the fillers, to be interacted with the nitrile

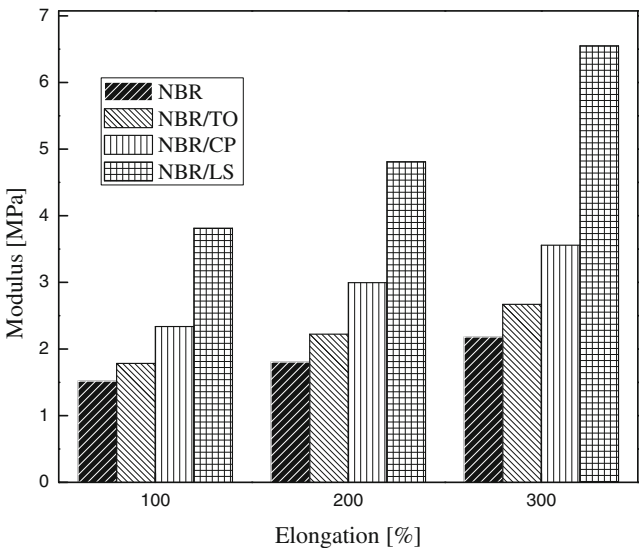

Fig. 7 Modulus enhancement at 20 phr filler loading of NBR/TO, NBR/CP and NBR/LS systems

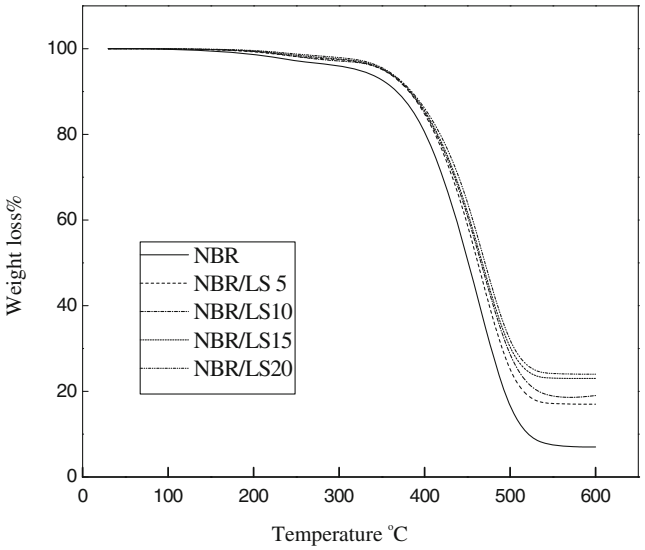

Fig. 8 TGA curves of layered silicate/nitrile rubber nanocomposites

rubber matrix. But in the case of layered silicate the high aspect ratio enables the filler to act as good reinforcing material with the polymer matrix. One can conclude that the thermal stability enhancement as a result of the addition of CP and TO follows almost similar path. It is generally believed that the inclusion of inorganic components into organic materials can improve their thermal stability [34]. The maximum onset degradation temperature with filler loading is displayed in Fig. 11. The graph revealed that highest degradation temperature is associated with layered silicate filled system, which is an indication of the better thermal stability of the system. Again, it can be observed from the graph that the thermal stability increased with the increase in filler content. This is due to the fact that the availability of surface area, because of high aspect ratio of the filler per unit volume of the matrix has been increased

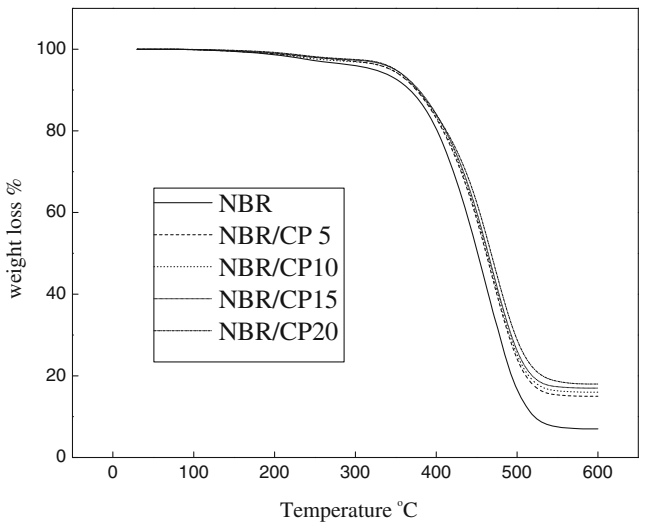

Fig. 9 TGA curves of Calcium phosphate/nitrile rubber nanocomposites

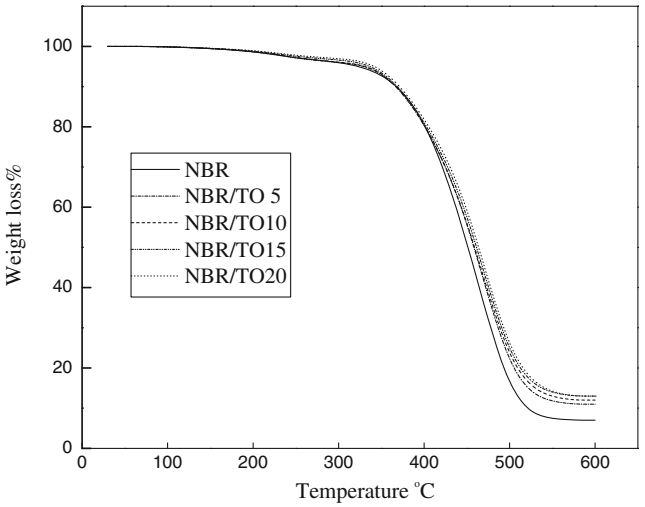

Fig. 10 TGA curves of Titanium dioxide/nitrile rubber nanocomposites

which acted as protective layer against the thermal degradation.

Kinetic parameters for thermal decomposition

The kinetic parameters for the thermal decomposition of nitrile rubber nanocomposites with fillers of different particle size and chemical nature were analyzed by applying an analytical method proposed by Coats–Redfern [35].

It is an integral method for the calculation of activation energy and the following equation is used

$$\log\left[-\frac{log\,(1-\alpha)}{T^2}\right] = \log\left\{\left(\frac{AR}{\beta E}\right)\left(1-\frac{2RT}{E}\right)\right\} - \frac{E}{2.303RT} \quad (1)$$

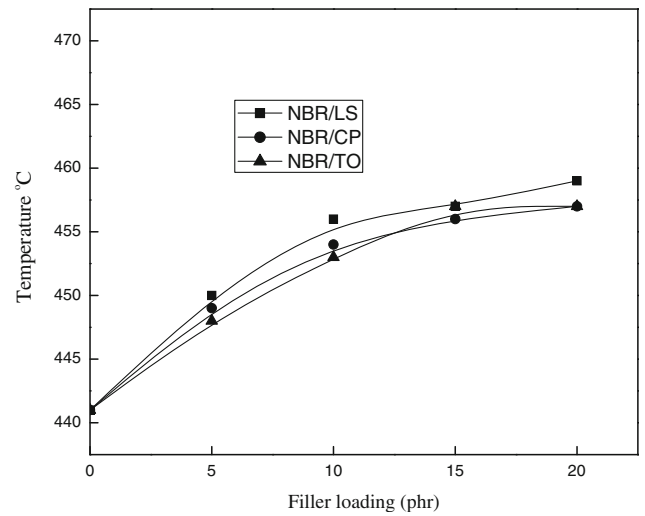

Fig. 11 Variation of maximum degradation temperature of NBR and nanocomposites with filler loading

where α is the decomposed fraction at any temperature and is given by the expression $\alpha = \frac{C_i - C}{C_i - C_f}$ where C is the weight; at the temperature chosen, Ci is the weight at the initial temperature and C_f is the weight at final temperature, β is the heating rate, E is the activation energy for decomposition. The activation energy and the pre-exponential factor (A) were determined from the plot of log $\{-\log(1-\alpha)/T^2\}$ against ($1/T$) which is shown in Fig. 12.

The activation energy values obtained for various filled nitrile rubber samples are presented in Table 2. From the data it can be inferred that the addition of nanofillers increases the activation energy, for the thermal degradation of the polymer. The higher value of activation energy is an indication of the relatively better thermal stability of the system. Noticeable increase in the activation energy value is observed in the case of layered silicate filled sample and it can be explained on the basis of strong intercalation/exfoliation of the polymer matrix with the filler. The exfoliation/intercalation pattern is also clear from the TEM pictures. This will result in the creation of a barrier effect of the silicate layers on the surface of the NBR matrix.

Table 2 Activation energy for the degradation of nanocomposites at 10phr filler loading

Sample	Activation energy (kJ/mol)
NBR	311.0
NBR/TO	324.8
NBR/CP	345.6
NBR/LS	355.9

Differential scanning calorimetric analysis (DSC)

In the case of polymer nanocomposites, the DSC measurements are useful for the identification of the extent of intercalation/exfoliation of the nanoparticles in the matrix. The segmental mobility of the polymer matrix is greatly affected by the interactions of the intercalated/exfoliated polymer chains with the nano fillers thereby increasing the glass transition temperature of the polymer. In the present study, DSC measurements were performed at a temperature range of –50°C to 90°C. The DSC curve of NBR showed the glass transition (Tg) at −19.51°C whereas the layered silicate nanocomposite showed the glass transition (Tg) at a higher temperature with an increase of 7.4° C (i e −12.11°C) at 10phr filler loading. The increase in Tg of the nanocomposites might be due to (i) the effect of a small amount of dispersed clay on the free volume of polymer and (ii) the confinement of the intercalated/exfoliated polymer chains within the clay galleries, which resists the segmental motion of the polymer chains as reported by Lu et al. [36]. The observed Tg values of CP and TO filled samples at 10phr loading are −16.24°C and −18.52°C respectively. Since the Tg values are an indication of segmental mobility of polymer in presence of fillers, the addition of layered silicate restricts the segmental mobility more effectively than TO and CP. This observation can be attributed to the effective intercalation of the layered silicate due its particle geometry. Figure 13 describes impact of filler addition on the glass transition (Tg) values of nitrile rubber nanocomposites. From the Tg values, it is clear that the overall intercalating efficiency of the filler with the matrix varies in accordance with the filler geometry. Filler with layered structure effectively intercalates with the matrix due to the availability of more surface area per unit volume producing considerable change in the Tg value in comparison with more spherical fillers. Hence based on the

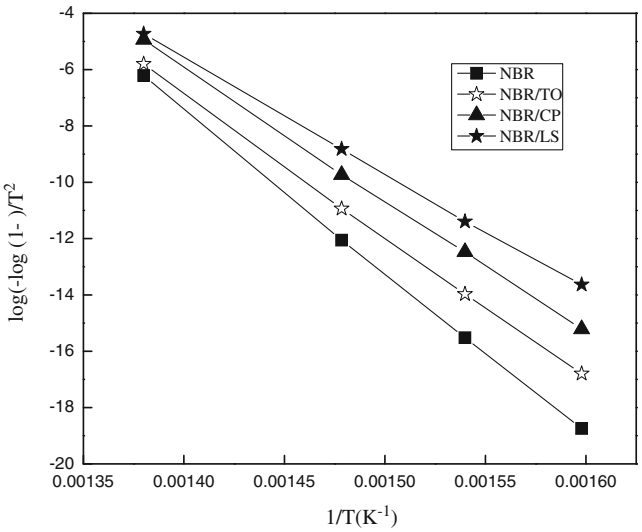

Fig. 12 Coats –Redfern plots of nitrile rubber nanocomposites at 10 phr filler loading

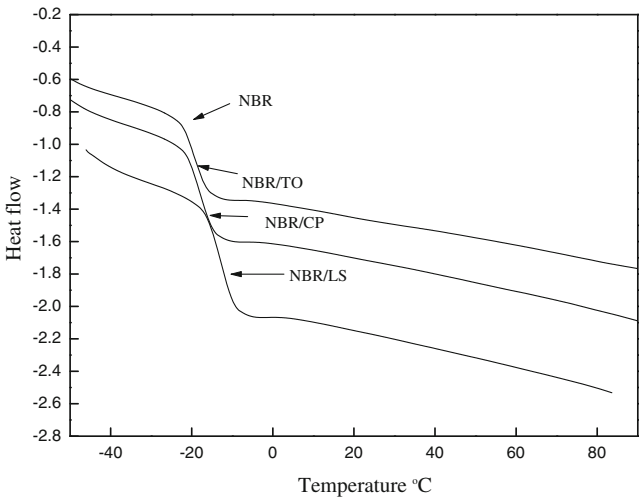

Fig. 13 DSC thermogram of NBR and nanocomposites with different fillers at 10 phr loading. (The glass transition temperature (Tg) of samples are indicated by arrows at a heating rate of 10° C/min)

filler geometry and Tg values, the intercalating efficiency varies in the order LS > CP >TO.

A plot of change in heat capacity (ΔCp) against filler loading is shown in Fig. 14. The ΔCp values obtained for different nanocomposites were correlated with the degree of reinforcement. It can be assumed that more polymer chains are attached on to the surface of the filler and there exists an immobilized layer around the filler surface and the layers do not take part in the relaxation process. A schematic representation is given in Fig. 15. The picture shows the relative abundance of nitrile rubber or polymer matrix on the surface of the layered silicate filler. The ΔCp value for NBR was calculated using the parameters from ATHAS databank and it was found to be 0.79. Our experiments also showed a similar result. The filler addition will naturally decrease the ΔCp values for the polymer, as fillers do not contribute anything towards specific heat capacity. Therefore the ΔCp value for filler is taken as zero. If there is no interaction between the filler and the polymer the composites should follow the linear path shown in the figure. However, it is not the case for the all the three filled systems. This is another reason indicating that there exists a strong interaction between the polymer matrix and layered silicate resulting out of the polar-polar reactive mechanism. Nitrile rubber being polar might be interacting with hydroxyl group present on the silicate filler thereby reducing the segmental mobility considerably. This is the reason why layered silicate filled sample showed minimum ΔCp value in comparison with CP and TO filled system.

Mathematical modeling

The overall mechanical property variations are associated with the loading of nano fillers having different particle size

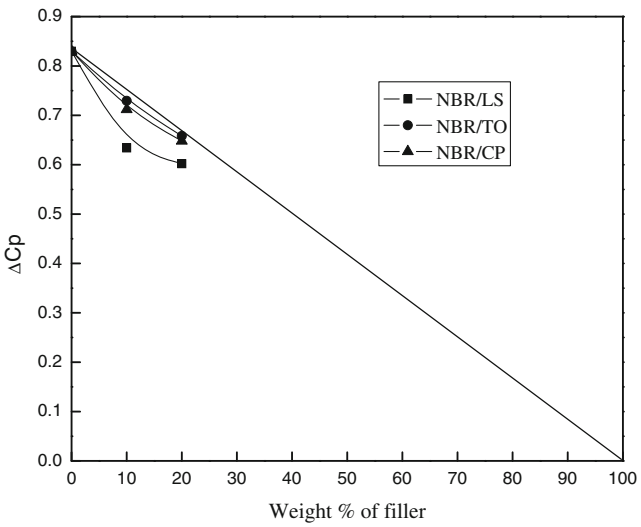

Fig. 14 Variation ΔCp (change in specific heat capacity) with filler loading

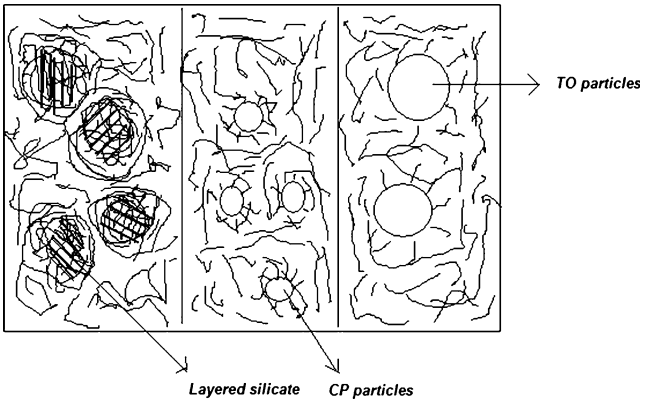

Fig. 15 Schematic representation of the relative abundance of polymer matrix on the surface of the filler

and these variations can be explained on the basis of particle geometries and their respective surface area to volume ratio. In the case of fillers the surface area per unit volume is inversely proportional to its diameter, thus, the smaller the diameter of a particle the greater the surface area per unit volume. The approximate surface to volume ratio of the filler can be calculated as follows [37].

For a spherical particle

$$\text{Surface area} = 4\pi r^2 \tag{2}$$

$$\text{Volume} = \frac{4}{3}\pi r^3 \tag{3}$$

Where r is the radius of the particle.

Hence surface area to volume ratio is $3/r$ which shows that particles with larger size (diameter) will provide less

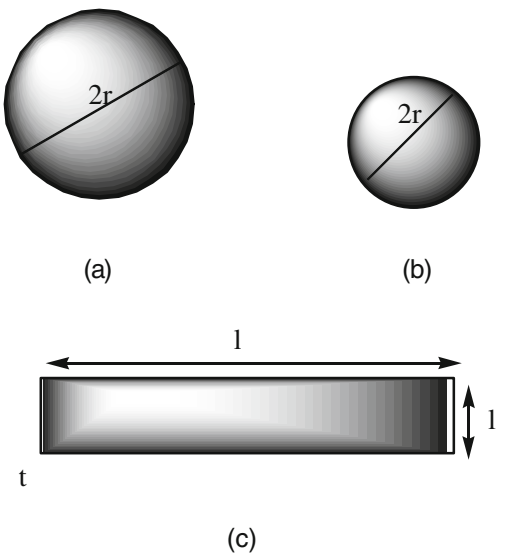

Fig. 16 Pictorial representation of the filler shape (**a**) TO and (**b**) CP with surface area/volume ratio is 3/r (**c**) Layered particle with surface area/volume ratio is $2/t + 4/l$

surface area per volume for interaction with the polymer matrix. This case is applicable with TO filled systems where large size of the filler particle reduces the availability of surface area per unit volume for interaction with the matrix resulting in poor tensile properties. The CP particles are comparatively small in size and hence by applying the above argument the availability of surface area per unit volume will be more; resulting in better tensile properties.

For a layered material,

$$\text{Surface area} = 2l^2 + 4lt \tag{4}$$

$$\text{Volume} = l^2 t \tag{5}$$

Where l is the length of the layered material and t is the thickness.

Here surface area to volume ratio is $2/t + 4/l$. The second term in the equation has very small influence compared to the first term and therefore it is often omitted. Therefore, logically, a change in particle diameter or layer thickness from micrometer to nanometer range will affect the surface area to volume ratio to a very large extent. The layered silicate having thickness in the nanometer range will have large surface area to volume ratio and therefore the availability of surface area per unit volume is higher in comparison with TO and CP. This enables a very good interaction with the polymer matrix resulting in enhanced tensile properties. Based on the above argument a pictorial representation can be given to the fillers having spherical and layered structures for their matrix filler interaction, which is represented in Fig. 16.

Conclusion

In this study NBR nanocomposites were successfully prepared by two roll mixing method using three different fillers, namely calcium phosphate, titanium dioxide and nano silicate. The XRD characterization of nanocomposites revealed the existence of intercalated/exfoliated structures. In comparison the nanoclay had a more pronounced impact on the mechanical and thermal properties of the NBR composites compared to TO and CP fillers. The TEM and AFM images revealed the presence of well-dispersed silicate layers in the NBR matrix in comparison with CP and TO fillers indicating further that the silicate layers had a more pronounced reinforcement effect on NBR compared to CP and TO fillers. NBR nanocomposites with fillers of different particle geometry exhibited enhanced mechanical and thermal stability in comparison with unfilled NBR. FTIR studies revealed the presence of strong interaction between layered silicate and polymer matrix and hence NBR nanosilicate composites showed very good mechanical and thermal properties. The enhancement in mechanical and thermal stability as a result of the incorporation of the fillers was attributed also due to the extent of the availability of surface area for strong interaction with the polymer matrix. Glass transition values showed a marginal change with the nature of the filler geometry. Fillers with layered structure reduced the segmental mobility more effectively than fillers with more spherical structure resulting in the minimum heat capacity value of the layered silicate filled system. Similarly the activation energy needed for the thermal degradation of the layered silicate filled sample is found to be higher than that of gum and other filled samples. The mathematical modeling of various fillers was also done and was found to be in agreement with the experimental results.

References

1. Pinnavai T (1983) J. Science 220:365
2. Alexandre M, Dubois P (2000) Mater Sci Eng 28:1
3. Rajan MAJ, Mathavan T, Ramasubbu A, Thaddeus A, Latha VF, Vivekanandam TS, Umapathy S (2006) J Nanosci Nanotech 6:3993
4. Bourbigot S, Gilman J, Wilkie CA (2004) Polym Deg Stab 84:483
5. Peng Z, Kong L, Xli SD, Spiridonov P (2006) J Nanosci Nanotech 6:3934
6. Mohan TP, Kumar MR, Velmurugan R (2006) J Mater Sci 41:5915
7. Ma CCM, Chen YJ, Kuan HC (2006) J Appl Polym Sci 100:508
8. Li SD, Peng Z, Kong LX, Zhong JP (2006) J Nanosci Nanotech 6:541
9. Valera-Zaragoza A, Ramirez-Vargas E, Medellin-Rodriguez FJ, Huerta-Martinez BM (2006) Polym Deg Stab 91:1319
10. Varghese S, Karger-Kocsis (2003) J Polymer 44:4921
11. Leszczynska A, Njuguna J, Pielichowski K, Banerjee JR (2007) Thermochim Acta 453:75
12. Wan T, Feng F, Wang YC (2006) Polym Bull 6:413
13. Wang LH, Sheng J (2006) J Macromol Sci – Phys B 45:1
14. Liufu SC, Xiao HN, Li YP (2005) Polym Deg Stab 87:103
15. Wang D, Zhu J, Yao Q, Wilkie CA (2002) Chem Mater 14:3837
16. Dongcheol C, Abdul Kader M, Baik-Hwan C, Yang-il H, Changwoon N (2005) J Appl Polym Sci 98:1688
17. Kader MA, Kim K, Lee YS, Nah C (2006) J Mater Sci 41:7341
18. Kim J-T, Oh T-S, Lee D-H (2003) Polym Int 52:1203
19. Nah C, Ryu HJ, Kim WD, Chang YW (2003) Polym Int 52:1359
20. Kojima Y, Fukumori K, Usuki A, Okada A, Kurauchi T (1993) J Mater Sci Lett 2:889
21. Wu Y-P, Jia Q-X, Yu D-S, Zhang L-Q (2003) J Appl Polym Sci 89:3855
22. Nah C, Ryu HJ, Han SH, Rhee JM, Lee MH (2001) Polym Int 50:1265
23. Kim JT, Oh TS, Lee DH (2004) Polym Int 53:406
24. Thomas SP, Thomas S, Abraham R, Bandyopadhyay S (2008) eXPRESS Polym Lett 2:528
25. Varghese S, Korger-Kocsis J, Gatos KG (2003) Polymer 44:3977
26. Arroyo M, Manchado L, Herrero B (2003) Polymer 44:2447
27. Hwang WG, Wei KH, Wu CM (2004) Polymer 45:5729
28. Passaglia E, Bertuccelli W, Ciardelli F (2001) Macromol Symp 176:299

29. Pramanik M, Srivastava SK, Samantaray BK, Bhowmick AK (2002) J Polym Sci Part B: Polym Phys 40:2065
30. Vu YT, Mark JE, Pham LH, Engelhardt M (2001) J Appl Polym Sci 82:1391
31. Han M, Kim H, Kim E (2006) Nanotechnology 17:403
32. Thomas SP, Joseph K, Thomas S (2004) Mater Letters 58:281
33. Shim H, Kim ES, Joo JH, Yoon JS (2006) J Appl Polym Sci 102:4983
34. Wen J, Wikes GL (1996) Chem Mater 8:1667
35. Coats AW, Redfern JP (1964) Nature 68:201
36. Lu H, Nutt S (2003) Macromolecules 36:4010
37. Farzana H, Mehdi H, Masami O, Russelle G (2006) J Compos Mater 40:1151